

## Simulated human eye retina adaptive optics imaging system based on a liquid crystal on silicon device

This article has been downloaded from IOPscience. Please scroll down to see the full text article.

2008 Chinese Phys. B 17 4529

(<http://iopscience.iop.org/1674-1056/17/12/033>)

View [the table of contents for this issue](#), or go to the [journal homepage](#) for more

Download details:

IP Address: 221.8.12.150

The article was downloaded on 11/09/2012 at 05:51

Please note that [terms and conditions apply](#).

# Simulated human eye retina adaptive optics imaging system based on a liquid crystal on silicon device\*

Jiang Bao-Guang(姜宝光)<sup>a)b)†</sup>, Cao Zhao-Liang(曹召良)<sup>a)b)</sup>, Mu Quan-Quan(穆全全)<sup>a)b)</sup>,  
Hu Li-Fa(胡立发)<sup>a)</sup>, Li Chao(李超)<sup>a)b)</sup>, and Xuan Li(宣丽)<sup>a)</sup>

<sup>a)</sup>State Key Lab of Applied Optics, Changchun Institute of Optics, Fine Mechanics and Physics,  
Chinese Academy of sciences, Changchun 130033, China

<sup>b)</sup>Graduate School of the Chinese Academy of Sciences, Beijing 100039, China

(Received 19 March 2008; revised manuscript received 12 May 2008)

In order to obtain a clear image of the retina of model eye, an adaptive optics system used to correct the wave-front error is introduced in this paper. The spatial light modulator that we use here is a liquid crystal on a silicon device instead of a conventional deformable mirror. A paper with carbon granule is used to simulate the retina of human eye. The pupil size of the model eye is adjustable (3–7 mm). A Shack-Hartman wave-front sensor is used to detect the wave-front aberration. With this construction, a value of peak-to-valley is achieved to be  $0.086\lambda$ , where  $\lambda$  is wavelength. The modulation transfer functions before and after corrections are compared. And the resolution of this system after correction (69lp/m) is very close to the diffraction limit resolution. The carbon granule on the white paper which has a size of  $4.7\mu\text{m}$  is seen clearly. The size of the retina cell is between 4 and  $10\mu\text{m}$ . So this system has an ability to image the human eye's retina.

**Keywords:** liquid crystal device, adaptive optics, ophthalmic optics

**PACC:** 4270D, 0760, 4278F, 4290

## 1. Introduction

Adaptive optics is a technology with the merit of real-time detection, real-time control and real-time correction. It is endowed with an ability to eliminate the dynamic disturbance, thereby obtaining clear images of the target. In 1953 adaptive optics was first suggested by Babcock<sup>[1]</sup> in astronomy to improve the performance of ground-based telescope. After his success, more and more systems were used in astronomy observation and laser communication.<sup>[2,3]</sup> Although a series of achievements has been acquired, this technology will not be used in physics and industry until the facility is made small enough.

Human eyes retina observation is significant in clinic ophthalmology, because not only the ophthalmic diseases but also other diseases such as the diabetes can be diagnosed by imaging the cell or the blood vessel of the retina. Although the retinoscope has been used for observation, we cannot obtain the cell image clear enough yet, except for pathology slice. Obviously the slice observation cannot be used in alive human.

The factors restricting the retinoscope resolution power is that the magnitude and the format of the wave aberration of human eye are various. The adaptive optics system is competent for this task because of its merit mentioned above.

At present, many research organizations incline to high resolution retina imaging,<sup>[4–9]</sup> but the corrector they are using is a deformable mirror. The deformable mirror has some merits such as high response speed, high light power efficiency, etc., but it has many disadvantages, such as high cost, high drive voltage, big bulk, and limited modulation range.

Compared with the conventional wave-front corrector deformable mirror, the liquid crystal on silicon device has the advantages, such as low costs, smaller size, reliability, low power consumption, high resolution, and high dynamic range with phase wrapping as mentioned in several papers.<sup>[10–14]</sup>

In this paper we introduce a simulated human eye retina imaging adaptive optics system based on a liquid crystal on silicon (LCOS) device, which has a small pixel pitch and high pixel density. Such a system

\*Project supported by the National Natural Science Foundation of China (Grant Nos 60578035, 50473040 and 60736042) and the Science Foundation of Jilin Province, China (Grant Nos 20050520 and 20050321-2).

†E-mail: jiangbg04@sina.com

is beneficial to imaging operations with a small area, high accuracy, large modulation depth, and high resolution. This will be helpful and necessary for human eye retina image with the liquid crystal modulator.

## 2. Optical configuration

A simulated human eye was built as shown in Fig.1. It was composed of white paper with carbon granule, an achromatic cemented double lens and a pinhole, which served as the retina, the lens and the pupil respectively. The focal length of lens L was 25 mm. The pupil diameter was adjustable in size and the carbon granule on the white paper was  $4.7\ \mu\text{m}$  which was as small as the cones. Owing to the dispersion of the liquid crystal,<sup>[15]</sup> we used a 532 nm laser as the source. We also used a laser diffuser to eliminate laser speckles. Based on this eye model we used an LCR2500 as a wave-front corrector and HASO32 as a wave-front detector.<sup>[14]</sup>

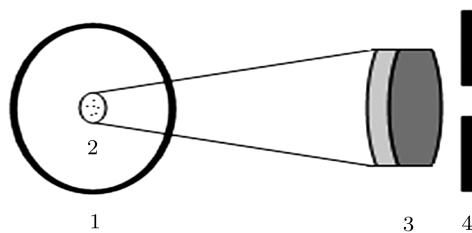


**Fig.1.** Eye model composed of white paper (1), carbon granules (2), double lens (3) and pupil (4).

Figure 2 shows the optical layout of the system. Light was irradiated from the laser source, the laser speckles were eliminated by the diffuser. The light power was collected by lens L1. After passing through the BS1 the light was focused by the lens L of the model eye.

We focused the light on the point at 250 mm away from the lens L. Then the light was further focused by the lens L2 (with a focal length of 100 mm) at a distance of 60 mm. Collimated by the lens L3 (with a focal length of 300 mm), the light was irradiated on the LCOS. The angle between the normal of the LCOS plane and the light axis was 3 degree. The light reflected by the LCOS was refocused by L3. A hole was located at the focus for eliminating other order diffraction light diffracted by the grating on the LCOS except for the first order.<sup>[16]</sup> Being collimated

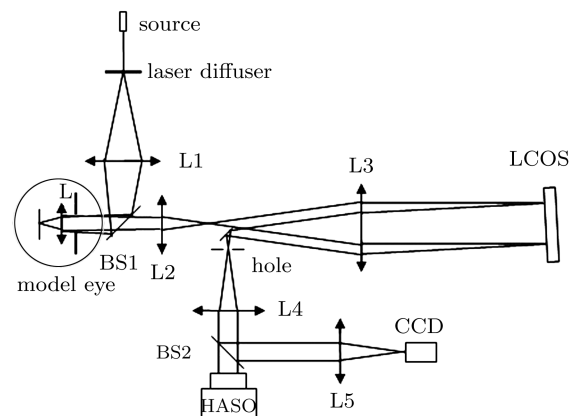


**Fig.2.** Schematic diagram of the system.

by the lens L4, the light was divided into two parts by the BS2, one was transmitted into HASO32 for detecting the wave-front aberration, and the other was focused on the image plane of the CCD for imaging. The LCOS plane was conjugated with the micro-lens array of the HASO, and the white paper was conjugated with the hole and the imaging plane of the CCD.

## 3. Results and discussion

For a real eye, medication can be used to enlarge the pupil size to 7 mm in diameter, which is the best diffraction limit. In this system, the image of the pupil on the LCOS plane was enlarged 3 times, and the active area of the LCOS was  $19.5\ \text{mm} \times 14.6\ \text{mm}$ . Being converted into the pupil position, the size of the active area is  $6.5\ \text{mm} \times 4.87\ \text{mm}$ . So the diffraction limit is determined by the size of the LCOS when the pupil size is 7 mm.

Images of the carbon granules before and after corrections and the corresponding wave-front maps are shown in Fig.3. When the close loop correction was steadily going, we made the voltage applied to the LCOS unchanged and replaced the whitepaper with a resolution test target. So we can estimate the imaging quality of the system after correction. We can clearly distinguish the sharpest line pairs on it, corresponding to 228 lp/mm. The aberration induced mainly by the roughness of the LCOS and the disturbance of the relevant environment are nearly  $2.6\ \lambda$  in PV value, where  $\lambda$  is wavelength and PV stands for peak-to-valley, and  $0.34\ \lambda$  in RMS, where RMS stands for root mean square, respectively. After close loop correction they reduce to  $0.086\ \lambda$  in PV value and  $0.016\ \lambda$  in RMS.

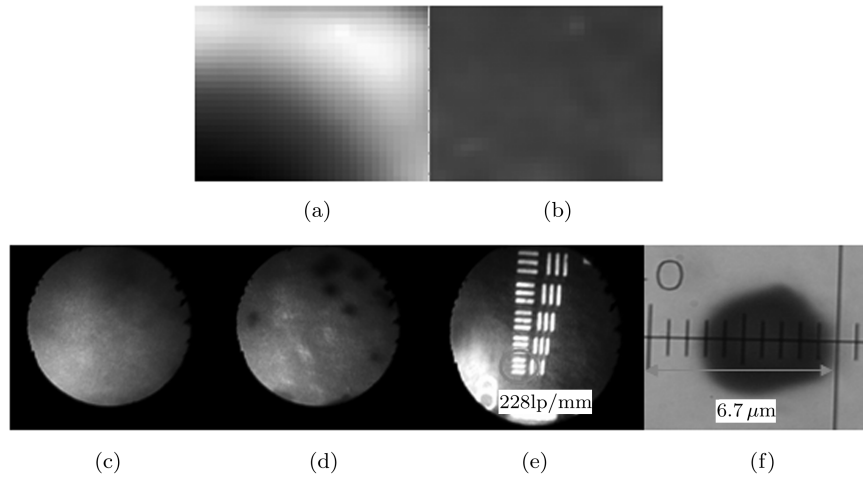


**Fig.3.** wave-front maps (a) before correction and (b) after correction ; images of the carbon granules (c) before correction and (d) after correction; (e) image of the resolution test target; (f) real size of the carbon granule at  $1000 \times 15$ .

The statistical curve is shown in Fig.4. We can see from these pictures that, after 321 times close-loop,

the system works steadily and effectively. The peaks are induced by the instability of the source.

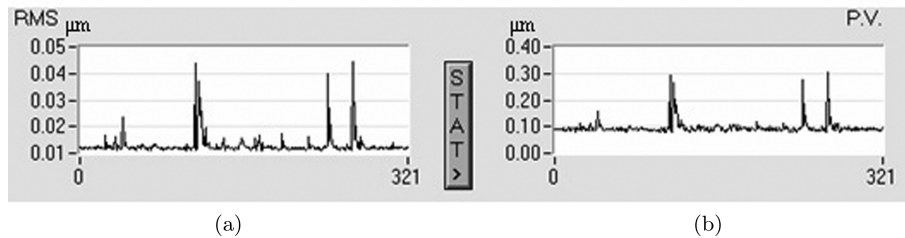


**Fig.4.** Statistical curves after 321 times close loop, where panel (a) is for RMS and panel (b) for PV value.

To evaluate the system, the modulation transfer functions (MTFs) are compared before and after the corrections. We assume the critical frequency to be 0.1. From Fig.5 it shows that the MTFs in both the

vertical and the horizontal directions are improved remarkably. In the horizontal direction the critical frequency increases from 40 to 70 lp/mm while the vertical one increases from 23 to 68 lp/mm. The difference

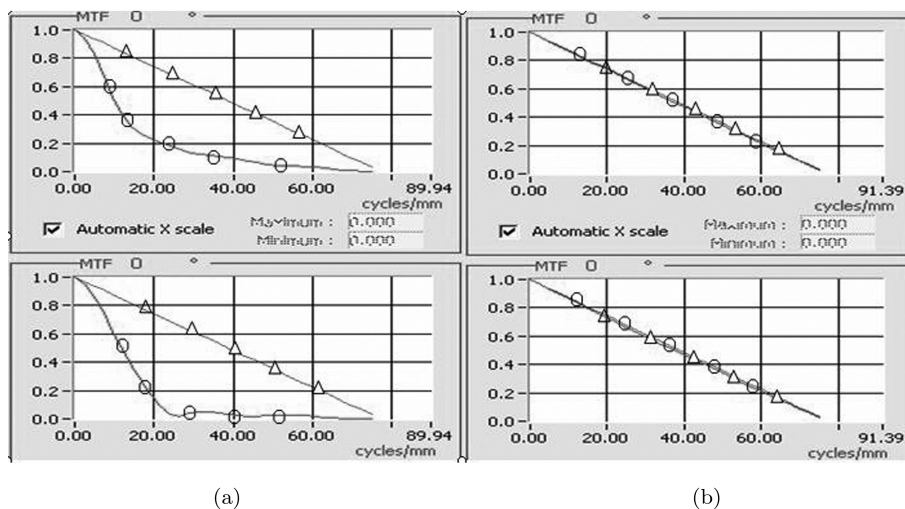


**Fig.5.** MTF curves before correction (a) and after correction (b).

between the horizontal direction and the vertical direction is due to the dimension of the LCOS (width: 19.5 mm height: 14.6 mm). They both approach the system diffraction limit.

In this optical system, the diffraction limit is determined by the diameter of the pupil of the model eye except for the case of 7 mm pupil size. So we made a series of close-loop corrections, with diameters of the pupil ranging from 3 to 7 mm. Figure 6 shows the critical frequency after correction and ideal values at different diameters. Figure 7 shows the PV value error and the RMS wave-front error before and after the corrections at different diameters.

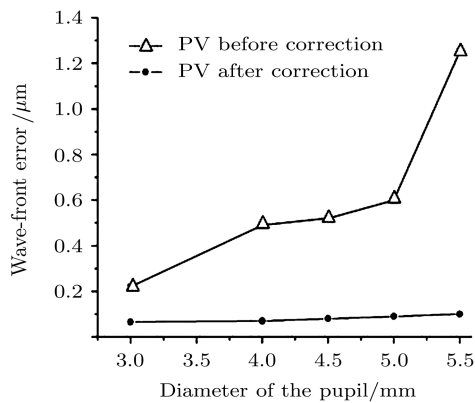


Fig.7. PV value errors and RMS wave-front errors before and after the corrections at different pupil diameters.

## 4. Conclusion

An adaptive optics retina imaging system based on liquid crystal on silicon<sup>[17]</sup> is demonstrated in this paper. Using the LCOS as a wave-front corrector and the HASO32 as a wave-front detector, we can obtain

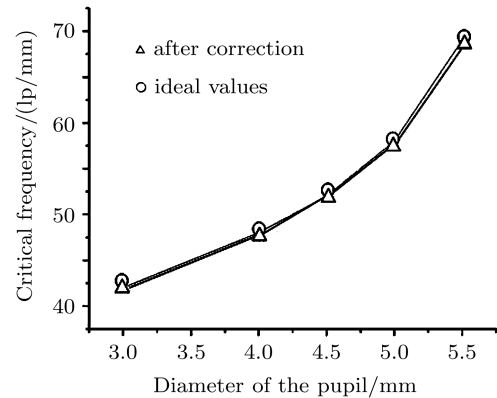
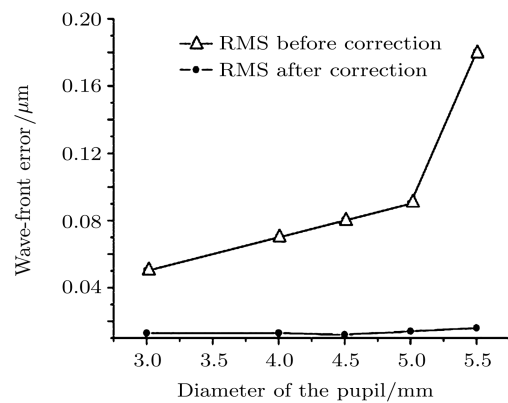


Fig.6. Critical frequencies after correction at different pupil diameters.



a series of clear images of the retina of the model eye in the case of various sizes of pupil. After close loop correction the aberration reduces to less than  $0.086 \lambda$  in PV value and  $0.016 \lambda$  in RMS and the diffraction limit resolution is approached in all cases.

## References

- [1] Babcock H W 1953 *Publ Astron. Soc. Pac.* **65** 229
- [2] Happer W 1994 *JOSA A* **11** 263
- [3] Gardner C S, Welsh B M and Thompson L A 1990 *Proc. IEEE.* **78** 1721
- [4] Liang J, Grimm B, Goelz S and Bille J 1994 *J. Opt. Soc. Am. A* **11** 1949
- [5] Liang J, Williams D R and Miller D T 1997 *J. Opt. Soc. Am. A* **14** 2884
- [6] Austin R and Fernando R B 2002 *Opt. Express* **10**
- [7] Enrique J, Fernandez and Pablo A 2003 *Optics Express.* **11**
- [8] Dubinin A, Belyakov A, Cherezova T and Kudryashov A 2004 *SPIE.* **55** 72
- [9] Ling N, Zhang Y, Rao X, Li X, Wang C, Hu Y and Jiang W *SPIE* **4825** 99
- [10] Cao Z, Xuan L, Hu L, Liu Y and Mu Q 2005 *Opt. Express* **13** 5186
- [11] Hu L, Xuan L, Liu Y, Cao Z, Li D and Mu Q 2004 *Opt. Express* **12** 6403
- [12] Martin F V, Prieto P M and Artal P 1998 *J. Opt. Soc. Am. A* **15** 2552
- [13] Mu Q, Cao Z, Hu L, Li D and Xuan L 2006 *Opt. Express* **14** 8013
- [14] Mu Q, Cao Z, Hu L, Li D and Xuan L 2007 *Opt. Express* **15** 1946
- [15] Li D, Mu Q, Hu L, Cao Z, Lu X and Xuan L *Acta Photon. Sin.* **6** 1065 (in Chinese)
- [16] Cao Z, Mu Q, Dovillaire G, Grandin T, Lavergne E, Hu L and Xuan L 2007 *Liquid Crystals* **34** 1227
- [17] Mu Q Q, Liu Y J, Hu L F, Li D Y, Cao Z L and Xuan L 2006 *Acta Phys. Sin.* **55** 1055 (in Chinese)